

Precast concrete double-tee connections, part 1: Tension behavior

Clay Naito, Liling Cao, and Wesley Peter

Precast concrete double-tees are commonly used for long-span floor systems in buildings and parking structures throughout the United States. Such systems are quick to erect, economical in cost, and help to resist lateral forces during seismic events. To provide integrity in the floor system, mechanical connectors are embedded in the double-tee flanges during manufacturing and are welded to adjacent double-tees during erection in the field. A precast concrete double-tee is typically fabricated with a 2-in.-thick (50 mm) flange and topped in the field with cast-in-place concrete or fabricated with a 4-in.-thick (100 mm) pretopped flange (**Fig. 1**).

For a regular floor diaphragm system spanning precast concrete frames or shear walls, the seismic demands on the joint connections are based on a girder analogy.¹ In this model, the diaphragm is assumed to act as a simple beam under a uniform load subjecting each joint to a combination of moment and shear. The connections at the boundary edges of the joint are designed to resist the tension and compression forces generated from bending of the diaphragm, and intermediate connections are designed to resist the shear within the diaphragm.

The connections located at the boundary edges are referred to as chord connections, and the connections placed between the chords are referred to as web connections. While the methodology provides a simple means for designing floor diaphragms, previous research has shown that conventional floor diaphragms are subjected to complex force and deformation demands under seismic events that are not effectively modeled by the girder analogy.²

Furthermore, because the girder analogy is a force-based design method, it does not account for the deformation capacity of the connection. In some cases, the web or chord connections may

Editor's quick points

- This paper shows that flange connections in topped diaphragm systems provide a high initial tensile resistance but provide the same response as an untopped system once the topping reinforcement fails.
- The strength of both chord and flange connections is over-predicted by PCI equations because of brittle modes of weld failure.
- Simplified models were developed to more accurately estimate the deformation capacity and strength.

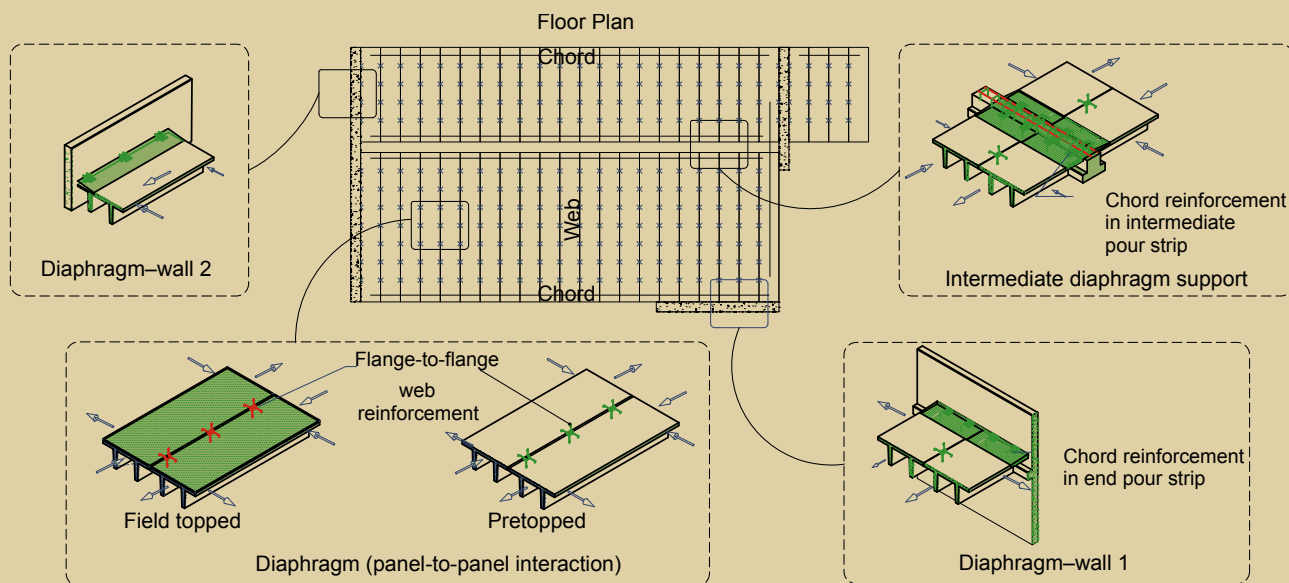


Figure 1. Precast concrete double-tees are typically fabricated with a 2-in.-thick (50 mm) flange and topped in the field with cast-in-place concrete or fabricated with a 4-in.-thick (100 mm) pretopped flange. Also shown are typical precast concrete double-tee diaphragm connections.

have limited deformability and result in premature failure of a floor diaphragm joint. To address these concerns, a collaborative research program has been conducted to develop a seismic design methodology for precast concrete diaphragms.^{3,4}

A key goal of the research is to characterize diaphragm connections from both a force- and displacement-capacity perspective. This allows for selective design of diaphragms by targeting a high deformation capacity while providing a combined shear and tension force resistance of both the web and chord connections in seismic regions where they are needed. This research program targets diaphragm connections commonly used by U.S. precast concrete producers. This paper presents the in-plane tension performance of pretopped and field-topped connection systems used in the U.S. precast concrete industry.

Industry survey of connection details

A wide variety of double-tee connections are in use by the precast concrete industry. To categorize common connections used in the United States, a survey of U.S. precast concrete producers and designers was conducted and the results are detailed in **Table 1**.⁵ Double-tee connection types are classified into three major categories:

- Category I: cast-in-place topping without an embedded connection
- Category II: cast-in-place topping with an embedded mechanical connection
- Category III: pretopped precast concrete double-tee with an embedded mechanical connection

In high seismic zones, engineers have relied on category I connections, which consist of a 2-in.-thick (50 mm) reinforced cast-in-place topping slab overlaying a 2-in.-thick precast concrete double-tee to ensure structural integrity. For these systems, reinforcing bars are used to provide continuity over the double-tees. As an alternative, systems consisting of a mechanical connection (category III) embedded in 4-in.-thick (100 mm) pretopped double-tee flanges are used. These systems are referred to as dry systems because they do not require the use of a field-placed topping. The embedded connection is typically field welded to the adjacent connection by a round or rectangular slug between the two exposed-steel-plate faces. Field erection requirements, such as leveling of the double-tees, often require the use of the welded mechanical connections even in low or moderate seismic regions. To provide a smooth and level floor surface, a combination of both a mechanical connection and cast-in-place topping (category II) is used.

In this paper, the embedded mechanical connections are classified in five subcategories based on their physical attributes (Table 1).⁵ Types DT1 through DT4 represent connections that can be fabricated from the reinforcing bar, plate, and angles. Category DT5 represents various proprietary connections that have been developed for use in precast concrete double-tees. Of the five connection types, bent reinforcing-bar connections (DT1) and proprietary connections (DT5) are the most popular web connections used in the United States for new construction. The pretopped or dry-chord connection consists of an embedded bar-to-plate connection (DT3). For topped conditions, continuous reinforcing bars are cast into the topping or into an elevated pour strip to provide the chord strength (Fig. 1).

Table 1. Double-tee connection details

<p>Embedded mechanical connectors</p>			
<p>DT1 embedded bent bar only</p>	<p>With recess</p>	<p>No recess</p>	<p>Vertical bent</p>
<p>DT2 continuous bar</p>	<p>Angle</p>		<p>Plate</p>
<p>DT3 embedded bar end welded to steel plate</p>	<p>Continuous across panel</p>	<p>Discontinuous</p>	<p>Angled legs</p>
<p>DT4 cover plate</p>	<p>Embedded steel plate</p>	<p>Embedded angle</p>	<p>Stud and bar anchorage</p>
<p>DT5 proprietary connectors</p>			

Note: 1 in. = 25.4 mm.

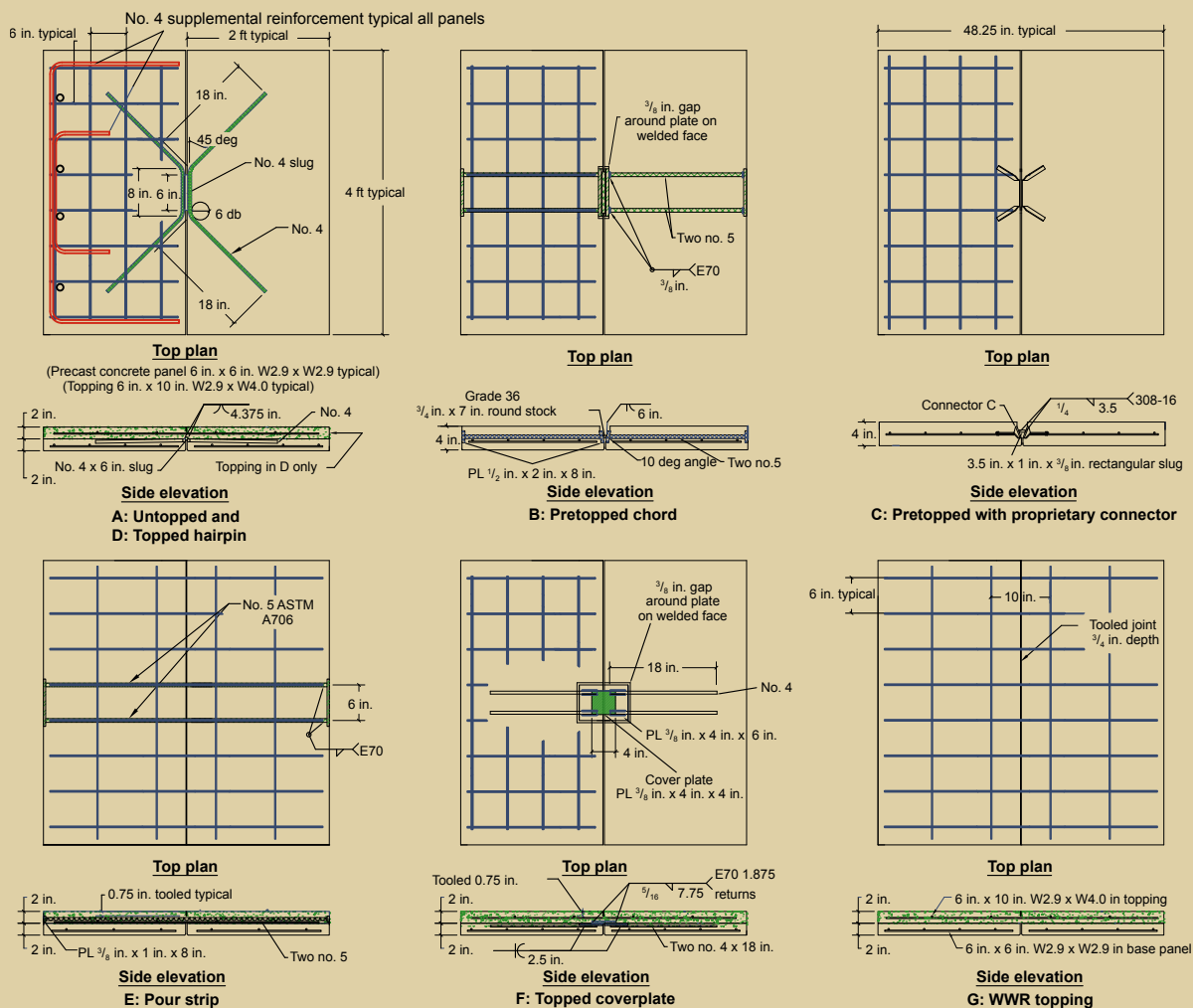


Figure 2. These specimen details are for the seven common connections selected from the industry survey for the experimental program. Note: ASTM = American Society for Testing and Materials; PL = plate; WWR = welded-wire reinforcement. No. 4 = 13M; no. 5 = 16M. 1 in. = 25.4 mm; 1 ft = 0.305 m.

Connection design and previous research

The force-based design method in *PCI Design Handbook: Precast and Prestressed Concrete*,¹ truss analogy, is used to compute the mechanical connection's tension capacity. This method assumes that the legs of the connector act in axial tension or compression to resist pullout. Adequate concrete strength is assumed but not checked in design. By equating the connection to an equivalent truss, the capacity is determined from the yield strength of the anchorage legs. Accordingly, the tensile force resisted by the legs is dependent on the leg orientation and the connector's material properties.

To evaluate the response of diaphragm connections, a significant amount of research has been conducted under in-plane demands. Venuti's⁶ tests on hairpin connections initiated the publication of studies in 1968 that have continued to the present with work by Oliva, Shaikh,

and others.⁷⁻¹⁵ As an initial step of the project, these past studies were quantified in a database of response curves.⁵ Examination of the existing data revealed that while the past research has been extensive, shortcomings remain with regard to the range of connections examined and the method of evaluation used.

The majority of research focused on the performance of web connections. Information on chord response was limited, and the contribution of the topping to the connection response has not been investigated. Furthermore, the goal of the majority of research was to determine the load-carrying capacity of the connection. As a consequence, the displacement capability was at times not clearly quantified.

To evaluate the diaphragm response during a seismic event, both the load resistance and the deformation capability of the individual web and chord connections must be known and be predictable. Unfortunately, current design recommendations are force based with no prescribed

guidance on how to estimate the displacement capacity. Consequently, an experimental program was developed to examine tension, shear, and combined shear with tension deformation demands on the individual web and chord connections.

Experimental program

Seven common connections (connections A to G) were selected from the U.S. precast concrete industry survey (Table 1) for the experimental program (Fig. 2). The specific details were developed in collaboration with an industry advisory board to duplicate current practice.¹⁶ Each connection was examined for both force and displacement capacities. One test per loading protocol was conducted for each connection specimen. The first phase of this study, presented in this paper, examined the tension response. The second phase of study, the shear response, will be presented in part 2 of this paper in *PCI Journal*.

The experimental subassembly replicates the boundary conditions of a typical embedded connection used between flanges of two adjacent precast concrete double-tees. The connection specimen consists of a pair of 2 ft × 4 ft (600 mm × 1200 mm) rectangular concrete panels with a connection cast at the center of one end of the panel. ACI 318-02¹⁷ temperature and shrinkage reinforcement in the form of welded-wire reinforcement (WWR) was used in each precast concrete panel. Two additional U-shaped no. 4 (13M) reinforcing bars were used to strengthen the boundary of the test subassembly (connection A in Fig. 2). Background information on each connection follows:

- Connection A is fabricated from a bent reinforcing bar (often referred to as a hairpin) belonging to category DT1 in Table 1. It has been used in 2-in.-thick (50 mm) untopped roof diaphragms for more than 40 years. Due to its low cost and ease of fabrication, it is one of the most common shear connections used in precast concrete structures. The straight front face of the hairpin is exposed on the vertical face of the double-tee flange and welded to an adjacent connection using a round slug to span the distance between panels. A minimum distance of twice the reinforcing-bar diameter measured from the weld toe to the bar bend is used to prevent embrittlement of the bar during welding.¹ An anchorage length of 18 in. (450 mm) is used to meet ACI 318-02 development length requirements; however, because the bar is angled into the flange, the initial shallow embedment will likely provide only a portion of the required amount.
- Connection B is used as both a dry-chord and web connection within 4-in.-thick (100 mm), pretopped, double-tee flanges and is commonly constructed from no. 4 (13M) or no. 5 (16M) reinforcing bars. The test specimen is fabricated from two no. 5 reinforcing bars

that are fillet welded to the exposed faceplate and installed in the panel prior to precast concrete operations. During erection, a round or square solid slug is installed between the adjacent faceplates and welded into place. To prevent the slug from dropping through to the floor below, the faceplate is angled backward at 10 deg. A slug of varying size is used in the field with the diameter chosen based on the gap available between the adjacent tees. The tested connection contains a 0.75-in.-diameter (18.75 mm) round stock with an effective throat of 0.2 times the bar diameter in accordance with American Welding Society (AWS) standards.¹⁸

- Connection C is a proprietary connection (DT5) commonly used by industry. The connector is fabricated from ASTM A304¹⁹ stainless-steel plate. This connection is commonly used in 4-in.-thick (100 mm), pretopped, double-tee flanges. A rectangular stainless-steel slug is attached between connectors with a fillet weld.
- Connection D is identical to connection A with the addition of 2 in. (50 mm) of topping and WWR meeting the ACI 318-02 temperature and shrinkage requirements.
- Connection E represents the chord reinforcement present in a 2-in.-thick (50 mm) topping slab placed over a 2-in.-thick, precast concrete, double-tee flange. This connection replicates the details used in a cast-in-place pour strip and is referred to as a *wet chord*. For this connection, two no. 5 (16M) reinforcing bars are used in combination with the minimum level of WWR. Two steel end plates are welded to the bar ends to artificially replicate the typical development length used.
- Connection F is a cover plate connection (DT4) commonly used for double-tee web or chord connections. The connection is welded using a rectangular plate and is topped with 2 in. (50 mm) of reinforced concrete and WWR. This connection is commonly used at diaphragm boundaries and can be installed as shown or on the underside of flanges to minimize patching of the floor.
- Connection G examines the contribution of field-placed topping to the joint strength. The size of WWR meets the minimum ACI 318-02 temperature and shrinkage reinforcement ratio requirement of 0.0018, per section 12.2.1 of chapter 17. WWR measuring 6 in. × 10 in. (150 mm × 250 mm) W2.9 × W4.0 is used, resulting in reinforcement ratios of 0.0024 and 0.0020. In addition, ACI 318-02 chapter 21 specifies that “the wires parallel to the span of the precast concrete elements shall be spaced not less than 10 in.

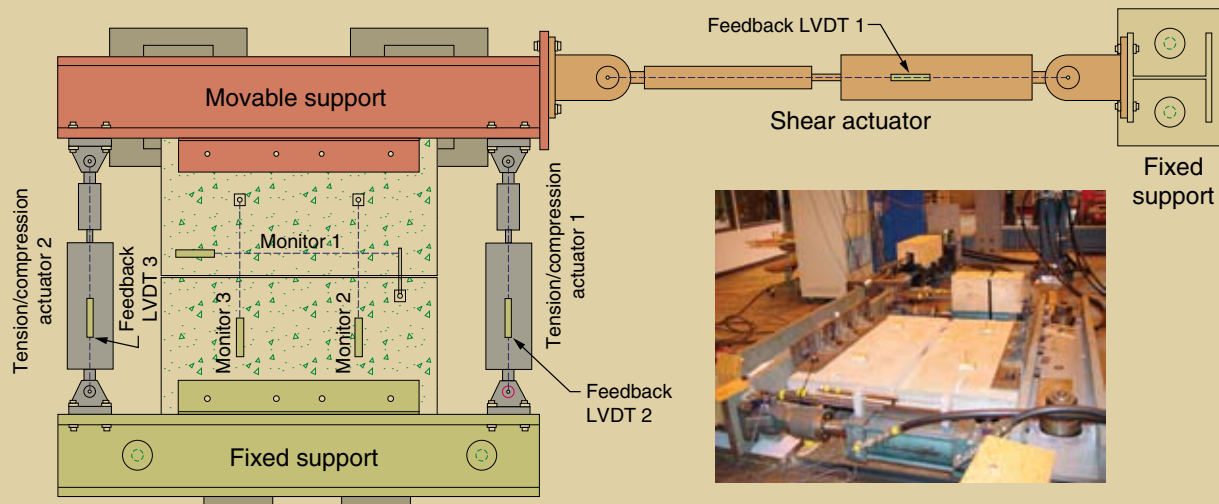


Figure 3. The multidirectional test fixture uses three actuators, two in the axial displacement and one in the shear displacement. Note: LVDT = linear variable differential transformer.

(250 mm) on center.” To accommodate this requirement, the WWR spacing across the joint was set at 10 in. and centered on the joint.

Material properties

Materials used for fabrication of the test specimens replicate the typical precast concrete construction. Self-consolidating concrete with a design strength of 7 ksi (48 MPa) was used for the precast concrete sections, and a conventional 4 ksi (28 MPa) ready-mixed concrete was used for the topping. Due to the low level of prestress present in conventional double-tee flanges, prestressing was not included in the specimens. Actual specimen concrete strength was measured from cylinder tests conducted according to ASTM C39.²⁰ Precast concrete compressive strengths averaged 7320 psi \pm 700 psi (50 MPa \pm 5 MPa), and the topping averaged 4110 psi \pm 510 psi (28 MPa \pm 3.5 MPa).

All steel plates were fabricated from ASTM A36 steel.²¹ Precast concrete panel and topping WWR conformed to the requirements of ASTM A185²² with a measured tensile strength of 105 ksi (725 MPa) and an ultimate strain capacity of 0.03. Reinforcing bars were made of ASTM A706²³ steel. Mill-certified yield and fracture strengths of no. 4 and no. 5 bars were 65.8 ksi (455 MPa) and 91.4 ksi (630 MPa), and 67.6 ksi (466 MPa) and 95.6 ksi (660 MPa), respectively. All welds were conducted using the shielded metal arc welding (SMAW) process using E7018 or 308-16 electrodes in accordance with AWS standards.²⁴

Test setup

A multidirectional test fixture was developed to allow for the simultaneous control of in-plane shear, axial, and bending deformations at the panel joint. The fixture uses three actuators, two in the axial displacement and one in the shear displacement (**Fig. 3**). Demand was applied through the independent displacement control of each of the three hydraulic actuators. The test specimen was connected to a restraint beam on either end of the panel. One beam was fastened to the lab floor, providing a fixed end, while the other beam rested on a pair of Teflon-coated steel plates, providing mobility with minimal frictional forces. Independent control of the three actuators allowed for application of shear, axial, and bending deformations. Vertical movement of the panel was restricted by Teflon-coated bearing pads under the center of each panel. This eliminated sag of the test specimen due to self-weight while still allowing for free, nearly frictionless travel in the horizontal plane of motion.

The joint deformation was measured directly on the precast concrete panel using a series of linear variable differential transformers (LVDT). These deformations were also captured by a series of feedback LVDTs on each actuator. Forces were measured using load cells in line with each actuator. The arrangement of displacement devices is illustrated in **Fig. 3**.

Loading protocol

The panels were tested under the pure tension deformation with the shear deformation and joint rotation prevented and under a combined tension with shear deformation. The tests were conducted under displacement control at quasi-static rates (<0.05 in./sec [<1 mm/sec]). Unless noted, all

panels were tested until the specimen capacity approached zero. Both monotonic and cyclic displacement protocols were used (Fig. 4). The cyclic protocol consisted of three cycles of tension and compression displacement at increasing levels of tension displacement. Each compression half cycle consisted of a displacement to 0.01 in. (0.25 mm).

Four elastic displacement levels were applied. The inelastic levels increased at a rate in accordance with a protocol developed for the Precast Seismic Structural Systems (PRESSS) program.²⁵ In the combined tensile and shear deformation tests, the ratio of tension deformation to shear deformation was kept constant and was applied in a monotonically increasing manner. The tension-to-shear deformation ratio was determined using finite-element modeling of typical diaphragm systems. The cover plate connection F was subjected to a ratio of 2.0. All other connectors were subjected to a ratio of 0.5.

Tension performance

Table 2 summarizes the results measured from the monotonic tension (MT) test, monotonic tension with shear

(MTV) test, and cyclic tension compression (CTC) test of seven connections. A four-point backbone curve in accordance with Federal Emergency Management Agency (FEMA)²⁶ recommendations is developed for each test as shown in Fig. 5. Point a is defined as occurrence of yield. For connections in which a yield point is not clearly defined, point a is defined as the point where the shear strength achieves 75% of peak resistance. Initial shear stiffness is calculated as the secant of strength-displacement relationship from origin to point a. Point b represents the peak load, and point c is defined as the point where the strength is less than 5% of the peak level. The points are defined in terms of the tension resistance T_a , T_b , and T_c , and the displacements Δ_a , Δ_b , and Δ_c . The tension stiffness K_t is the secant at point b. The measured tension resistance divided by the estimated strength P_n is tabulated for comparison. The formulations used for design estimates and discussions are presented in the next section.

The connections exhibited a significant range of strength and ductility. Figure 6 summarizes the MT, MTV, and CTC load-deformation response of each connection. Envelopes of the MT, combined MTV and CTC load-

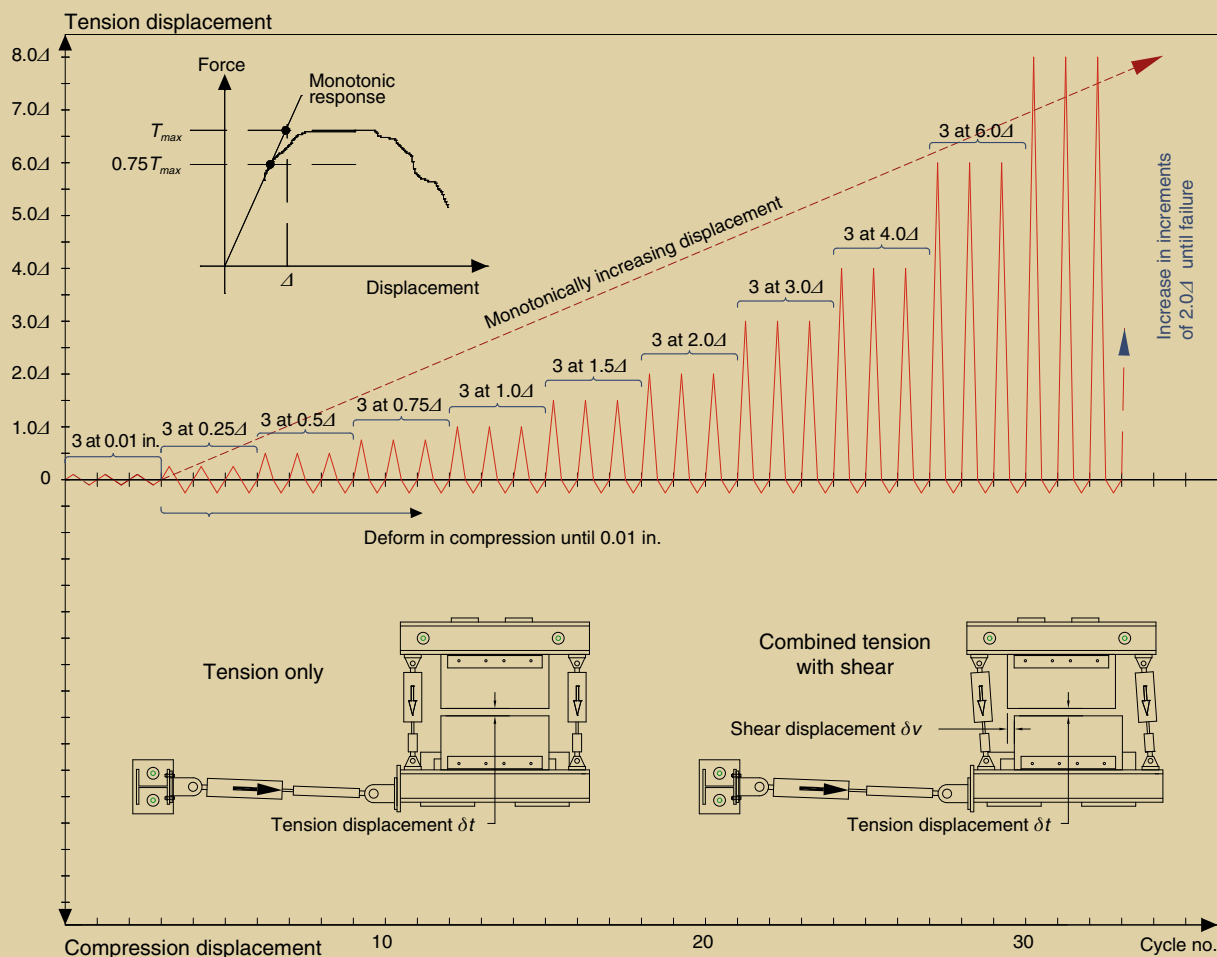


Figure 4. Both monotonic and cyclic displacement tension/compression protocols were used. Note: 1 in. = 25.4 mm.

Table 2. Test results

ID	Test type	a			b		c		P_n kip	T_b/P_n
		K_T kip/in.	Δ_a in.	T_a kip	Δ_b in.	T_b kip	Δ_c in.	T_c kip		
A	MT	45	0.120	2.60	1.440	7.71	1.850	1.83	17.00	0.454
B	MT	869	0.040	19.88	0.320	36.37	0.920	20.67	37.20	0.978
	MTV ($\delta_v/\delta_t = 2$)	622	0.020	10.26	0.370	33.78	0.430	23.57	37.20	0.908
C	MT	98	0.060	5.73	1.260	9.69	2.000	4.86	16.20	0.598
	CTC	48	0.065	3.14	0.498	5.90	0.752	4.41	16.20	0.364
D	MT	1128	0.014	15.80	0.048	25.00	1.696	6.06	32.10	0.779
	MTV ($\delta_v/\delta_t = 2$)	738	0.019	13.96	0.099	20.88	0.141	15.19	32.10	0.651
E	MT	1272	0.029	36.90	0.137	62.31	2.229	31.81	52.28	1.192
	MTV ($\delta_v/\delta_t = 1/2$)	755	0.047	35.49	0.149	59.42	2.166	54.77	52.28	1.137
	CTC	1151	0.042	48.36	0.119	62.58	0.833	49.79	52.28	1.197
F	MT	1406	0.023	32.34	0.148	43.42	0.566	26.57	39.08	1.111
	MTV ($\delta_v/\delta_t = 2$)	1252	0.020	24.43	0.050	27.17	1.480	8.94	39.08	0.695
G	MT	560	0.035	19.42	0.083	24.86	0.157	17.96	15.08	1.452
	MTV ($\delta_v/\delta_t = 2$)	297	0.064	19.04	0.084	21.89	0.115	15.83	15.08	0.454

Note: CTC = cyclic tension-compression; MT = monotonic tension; MTV = monotonic tension with shear. 1 in. = 25.44 mm; 1 kip = 4.448 kN.

deformation response are superimposed on the measured response for comparison purposes. The chord connections B, E, and F provided relatively high tension resistance, while the web connections A, C, and D and the topping G provided moderate resistance. The connections using field welds tended to initiate tearing at those locations, while the nonwelded connections typically necked and fractured near the joint. **Figure 7** presents these damage states.

Test observations

In general, tensile displacement of connections A, B, C, and D resulted in bending at the exposed front face. This produced large tensile deformations and a failure mechanism at the slug-to-connector weld region. These connections did not achieve their expected load-carrying capacity using a PCI truss analogy method. Furthermore, the tensile strength and flexibility of connections varied in accordance with the location, length, and size of weld used between the connector and the slug. Connections E, F, and G consisted of fracture of the topping WWR followed by fracture of the connection bars. Each of these connections met the expected design capacity. A detailed discussion of each connection follows:

- The untopped hairpin connection (A) exhibited bending of the unwelded hairpin bar portion outside of the weld followed by a fracture initiating from the root of the slug weld at 0.7 in. (17.5 mm) tensile displacement. The fracture propagated into the bar, resulting in a decrease in the load-carrying capacity and complete bar failure at 1.8 in. (45 mm).
- Connection B, the welded chord, exhibited cracking of the concrete above the embedded bars at 0.2 in. (5 mm) perpendicular to the joint, indicative of bond slip. This was followed by minor bending of the

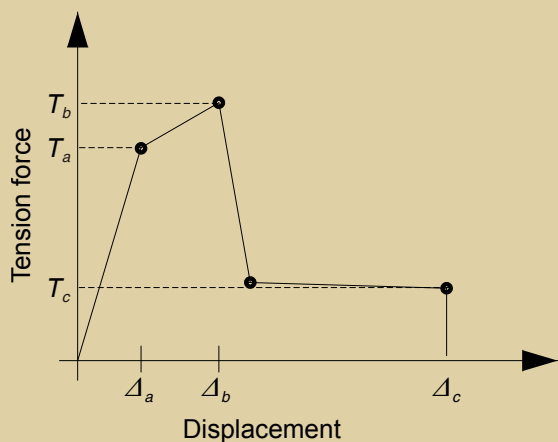


Figure 5. A simplified response curve was developed for each test in accordance with Federal Emergency Management Association 273 recommendations. Source: Building Seismic Safety Council 1997.

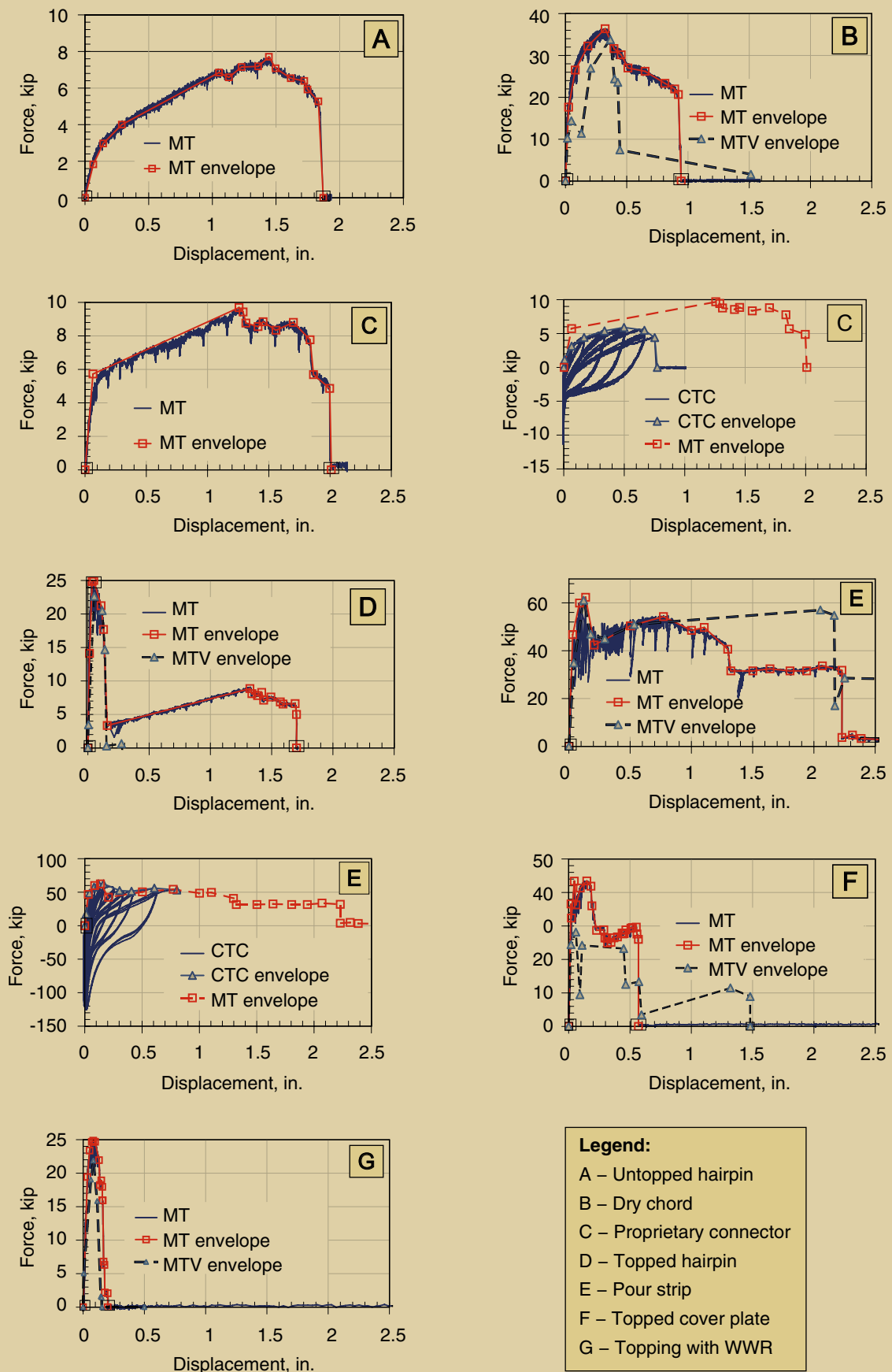


Figure 6. These graphs summarize the MT, MTV, and CTC load-deformation response of each connection. Note: CTC = cyclic tension-compression; MT = monotonic tension; MTV = monotonic tension with shear; WWR = welded-wire reinforcement. 1 in. = 25.4 mm, 1 kip = 4.448 kN.

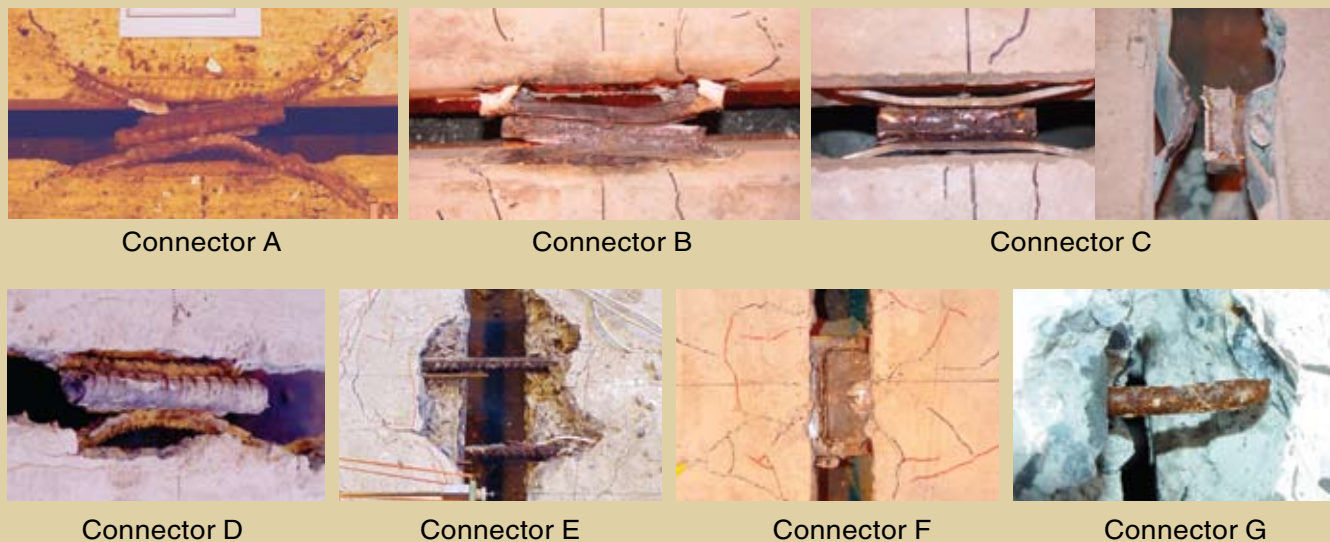


Figure 7. These photos show the damage caused under tension. The connections using field welds tended to initiate tearing at those locations, while the nonwelded connections typically necked and fractured near the joint.

connection front face and fracture at the connection-to-slug weld at 0.4 in. (10 mm) tensile displacement. Fracture propagated in the weld material producing appreciable plate bending and a decrease of the load-carrying capacity. The connection was lost at 0.9 in. (22.5 mm) due to fracture of the anchorage bars at the rear of the plate. The addition of a proportional shear deformation to the connection increased demands on the anchorage bars, resulting in bar fracture at 0.37 in. (9.25 mm) tensile displacement with 0.89 in. (22.25 mm) shear.

- Connection C, the proprietary connection, exhibited bending of the front face adjacent to the slug at both ends of the slug, followed by spalling of the concrete in front of the anchorage legs. Fracture of the slug-to-connection weld initiated in the weld material at 1.3 in. (32.5 mm) tensile displacement. Fracture propagated along the weld, resulting in complete loss of the connection at 2 in. (50 mm). Cyclic loading on this detail reduced the ultimate strength and deformation capacity over the monotonic response.
- Connection D, the field-topped hairpin, exhibited a stiff initial response due to the presence of the topping. Joint cracking initiated with application of joint opening. This was followed by elastic elongation, yielding, and fracture of the WWR at the joint. The WWR failed at 0.2 in. (5 mm) tensile displacement. Bending of the unwelded hairpin bar portion outside of the weld was observed, followed by fracture of the slug weld and progression through the hairpin at 1.7 in. (42.5 mm). Shear combined with tension placed more demand on the anchorage legs, resulting in a bar fracture initiated from the slug-to-bar weld.
- Connection E, the wet chord, exhibited cracking around the connection at the panel joint and fracture of the WWR in the topping by a tension opening of 0.2 in. The chord reinforcement reached its fracture strength, with one bar failing at the joint and the other within the topping. The addition of shear demand did not alter the tensile failure mode. The tensile force and deformation capacity with the proportional shear is about the same as that without shear.
- Connection F, the topped cover plate, formed local cracks around the connection, both in the topping and precast concrete panel. Fracture of the WWR was observed from 0.2 in. to 0.4 in. (5 mm to 10 mm), followed by tensile fracture of the two no. 4 anchorage bar legs at the end of the weld region at 0.6 in. (15 mm) tensile displacement. The presence of proportional shear produced rotation of the connection about the joint, which generated unequal tension demands on the anchorage bars. Tension capacity was compromised by concurrent shear, and fracture occurred at a lower deformation than the pure tension case.
- Connection G failed due to fracture of the WWR at the joint interface. No other damage was observed. Fracture occurred over a range of joint tensile displacement from about 0.1 in. to 0.2 in. (2.5 mm to 5 mm). Combined application of shear and tension decreased the force and deformation capacity from the pure tension test.

Strength estimates

The measured strength is compared with the nominal strength. The connections are intended to form a ductile tensile mechanism in the anchorage bars. All other components, such as the faceplate and slug weld, are designed with overstrength to prevent premature failure. To compare the measured results with the nominal strength, the mill-certified material properties of the reinforcing bar are used.

The formulations are generated from a simplified truss analogy in accordance with *PCI Design Handbook* section 3.6.2.¹ This force-based method estimates the available capacities due to a ductile failure in the connection leg. The welds were adequately proportioned to resist the bar fracture strength. Tension forces are applied uniformly and concentrically to the connection. In computing the tensile strength of the topped connections, it was assumed that the WWR and embedded connection both achieved yield; however, for the ultimate capacity the WWR was assumed to be fractured. Based on experimental observations, the assumptions of WWR deformations are appropriate.

The following notations are used:

- cross-sectional area of one leg of the connection A_s
- reinforcing-bar yield f_y or tensile strength f_u
- total cross-sectional area of WWR crossing the joint A_{wwr}
- WWR yield strength f_{wwr}

Table 3 summarizes the formulations and the computed nominal and ultimate strength of each connection.

The connections using the slug and weld (A through D) did not achieve the predicted nominal capacities (Table 3).

Their inability to meet their expected capacity is attributed to fracture of the weld as discussed in the test observations. The welding details used in these connections must be enhanced if they are to be relied on for tension resistance.

The pour strip (E), cover plate (F), and topping WWR (G) exceeded their predicted nominal and ultimate strengths. The lack of a welded connection at the joint in connections E and G allowed the wires and bars to achieve their full strength. The connection F weld detail allowed for full development of the anchorage bars under tension. Combined shear and tension deformation on the cover plate connection (F), however, produced nonsymmetrical demands on the bars, resulting in a premature failure of the connection.

Relative deformability of connections

The connections tested exhibited a wide range of tension stiffness. The untopped hairpin (A) and proprietary connection (C) exhibited a low tensile stiffness, while the chord connections (B and E) exhibited a stiff response. The WWR (G) provided moderate stiffness, while the topped connections provided high tensile stiffness (D, E, and F). The cover plate connection (F) provided the most rigid connection between panels.

The initial stiffness of the chord and web connections has a direct effect on the diaphragm response under earthquake and thermal loads. Because all of the connections along a diaphragm joint are in parallel, the forces will flow through the stiffest element. For example, for a typical diaphragm constructed from type C web connections and type B chord connections, the chord is more than eight times stiffer than the web connections.

For this system, tensile openings generated from earthquakes or temperature effects would result in tension forces eight times greater at the chord than at each web

Table 3. Truss analogy capacity estimates

Connector	Nominal capacity P_n , kip		Ultimate capacity P_{ult} , kip		Measured capacity T_B , kip
A: Untopped hairpin	$2(f_y A_s \cos 45)$	17.0	$2(f_u A_s \cos 45)$	25.8	7.71
B: Dry chord	$2(f_y A_s)$	37.2	$2(f_u A_s)$	59.3	36.37
C: Proprietary	$2(f_y A_s \cos 45)$	16.2	$2(f_u A_s \cos 45)$	32.0	9.69
D: Topped hairpin	$2(f_y A_s \cos 45) + f_{wwr} A_{wwr}$	32.1	$2(f_u A_s \cos 45)$	25.8	25.00
E: Pour strip	$2(f_y A_s) + f_{wwr} A_{wwr}$	52.3	$2(f_u A_s)$	59.3	55.00
F: Topped cover plate	$2(f_y A_s) + f_{wwr} A_{wwr}$	39.1	$2(f_u A_s)$	36.6	43.42
G: Topping	$f_{wwr} A_{wwr}$	15.1	$f_u A_{wwr}$	24.0	24.86

Note: A_s = cross-sectional area of one leg of the connection; A_{wwr} = total cross-sectional area of welded-wire reinforcement crossing the joint; f_u = reinforcing bar ultimate tensile strength; f_{wwr} = welded-wire reinforcement yield strength; f_y = reinforcing bar yield strength. 1 kip = 4.448 kN.

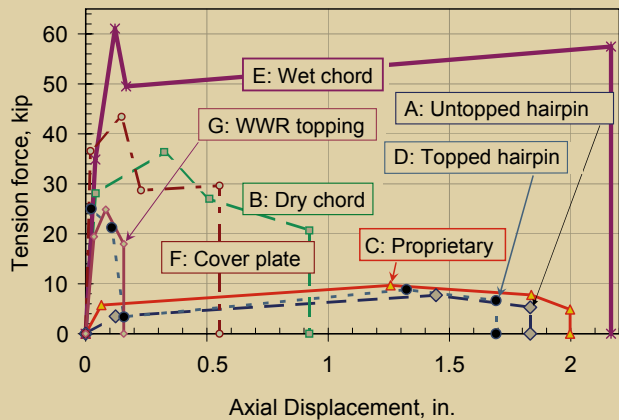


Figure 8. This graph shows the comparative response of connections. Note: WWR = welded-wire reinforcement. 1 in. = 25.4 mm; 1 kip = 4.448 kN.

connection. For floor systems in which the relative stiffness of connections is significantly large, the tensile contribution of the web connections should not be considered unless a deformation-based approach is used.

The majority of the connections exhibited nonductile characteristics. As illustrated in **Fig. 8**, the connections achieved their peak load capacity at a low deformation, 0.2 in. to 0.5 in. (5 mm to 12.5 mm). The proprietary and untopped hairpin connections were exceptions to this behavior, providing considerable deformability with an increased strength. The implication of this deformability is that the tension capacity of the web connection would not be achieved until significant tensile displacements of the joint had occurred. Consequently, the dry chord would have failed prior to achieving the hairpin tension strength.

To account for the combined strength of the web and chord, the connections must be designed to achieve their design strengths at similar levels of deformation. This can be achieved by development of a ductile chord that supports the design load over a large deformation range or through the use of stiff web connections that reach their design strength at the same deformation level as that of the chord. In any other case, reliance on the web connections for tensile resistance may result in an unconservative design.

Cyclic effects

Cyclic tension tests were conducted on the pretopped web connection (C) and the wet-chord connection (E). Figure 6 summarizes the cyclic responses. Cyclic loading of the welded web connection (C) resulted in a decrease in the force and deformation capacity. Slug-to-connection weld fracture occurred earlier than the monotonic test, achieving 38% of the monotonic deformation. This was attributed to low cycle fatigue of the weld material, resulting in the reduced tensile resistance and deformability of the connection.

Cyclic tensile behavior of the wet-chord connection (E) was in good agreement with the monotonic response. Unfortunately, failure of boundary support in the form of concrete breakout occurred at 0.83 in. (20.75 mm), preventing any further comparison after this deformation level. Prior to this level, compression loading produced buckling of the bar at the joint. This effect is observed in the pinching of the hysteresis curve of Fig. 6.

WWR topping contribution

When topping was used, the WWR contributed to the initial tensile response, providing an increase in the stiffness and strength. These properties, however, were quickly lost and the strength of the connection returned to that of an untopped condition.

The topping on its own was examined in connection G. As shown in Fig. 6 and Fig. 8, the WWR provided a moderate tensile resistance with the low deformation ductility. The measured strength matched the expected capacity computed from the tensile strength of the wires. In the United States, WWR is commonly produced by cold working large-diameter wire to the required WWR diameter needed. As a result of the cold-working process, the ductility of the material is significantly reduced, leaving limited deformation capacity available. The tensile strain capacity of wire ϵ_u can be computed using the formulation in Eq. (1) developed by Mirza and MacGregor:²⁷

$$\epsilon_u = 0.105\sqrt{\text{Area of wire}} \geq 0.0075 \quad \text{Eq. (1)}$$

Assuming that the smooth W2.9 wires have a gauge length equal to the transverse spacing of 10 in. (250 mm), the wires would theoretically fracture at 0.18 in. (4.5 mm). The test observations indicated that the wires fractured around this displacement level, as expected. Tensile deformation and strength are predictable, and the contribution of WWR to the joint capacity can be directly accounted for in the diaphragm design. The applicable range of deformation, however, must be considered and the contribution must be used only in instances in which the tensile displacement of the joint is expected to be less than 0.2 in. (5 mm).

The contribution of the topping was notable. For each topped connection, a sharp increase in the resistance was observed up to a deformation of 0.2 in. Once the WWR deformation capacity was exceeded, the resistance matched that of the untopped connection. This behavior is illustrated by comparing connections A and D in Fig. 8. The initial tension stiffness provided by the topping, however, did not directly add to the stiffness of the previously untopped connection.

For example, connection D, which was composed of a 2 in. (50 mm) topping and a hairpin, produced an initial

stiffness of 1128 kip/in. The addition of the stiffness from the topping and hairpin connections tested separately in A and G was only 605 kip/in. This indicates that the topping may provide confining effects to the hairpin connection, which allows it to achieve a higher combined stiffness when fabricated together.

Design recommendations for existing connections

As discussed previously, the measured tension response indicates that the strengths of connections A, B, C, and D are overpredicted by the *PCI Design Handbook* truss analogy. To address these observations, improved modeling recommendations are presented for the hairpin and dry-chord connection.

Hairpin connection (A and D)

As observed in tension testing, the nonwelded front region of the connection displaces flexibly under direct tension (Fig. 7). Flexibility of this region between the weld root and the hairpin bend governs the connection tension response. As a result of the lack of restraint, large tension deformations in excess of 1.5 in. (38 mm) are possible (Fig. 8). This observed behavior is used as a basis for a flexural mechanism model that can be used to determine the force and deformation capacity of the hairpin.

A simplified beam model is proposed as shown in Fig. 9. The beam length is equivalent to the connection front region between two bends (points A and D) while transverse loads are assumed to be uniformly distributed along

the equivalent length of the slug-to-plate weld (points B to C). The flexural stiffness at the bends is assumed to be minimal due to the lack of embedment, and the boundaries of the simple beam are assumed to be simply supported. Shear demands are neglected because the unwelded bar length is sufficiently larger than the depth of the bar.

The yield strength of the connection T_y is computed based on equilibrium of a free body diagram of the segment CD or AB when the plastic moment M_p is achieved at hinge locations of B and C. The plastic moment for a round bar can easily be determined from Eq. (2) by using the strength of materials, including the yield stress of the material F_y and the diameter of the bar d .

$$M_p = F_y \left(\frac{d^3}{6} \right) \quad \text{Eq. (2)}$$

Using this approach, the tension yield strength is estimated to be 2.2 kip (9.8 kN) for connection A. This is in good agreement with the measured yield of 2.6 kip (11.5 kN). This method can be used to conservatively estimate the nominal tension resistance of hairpin connections at moderate joint tension openings. At large openings, the deformed shape of the connection approaches a truss analogy as illustrated in Fig. 9. The predictability of this mechanism is questionable due to the potential for fracture propagation from the root of the slug weld into the bar, as observed in the tests (Fig. 9).

The tension stiffness can be modified based on the detailing used. If a minimum spacing is used between the slug

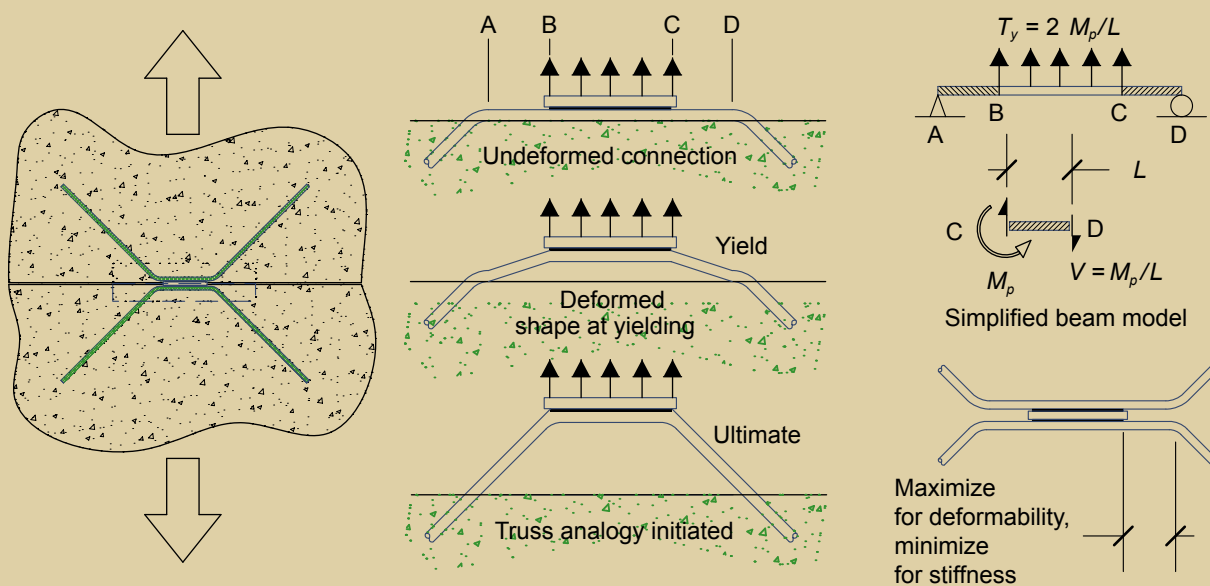


Figure 9. This simplified beam model was proposed. Also shown are the hairpin, undeformed connection, deformed shape at yielding, truss analogy initiated, and detailing for the proposed beam model. Note: L = distance from end of slug weld to bar bend; M_p = plastic moment; T_y = yield strength of the connection; V = shear in hairpin at yield.

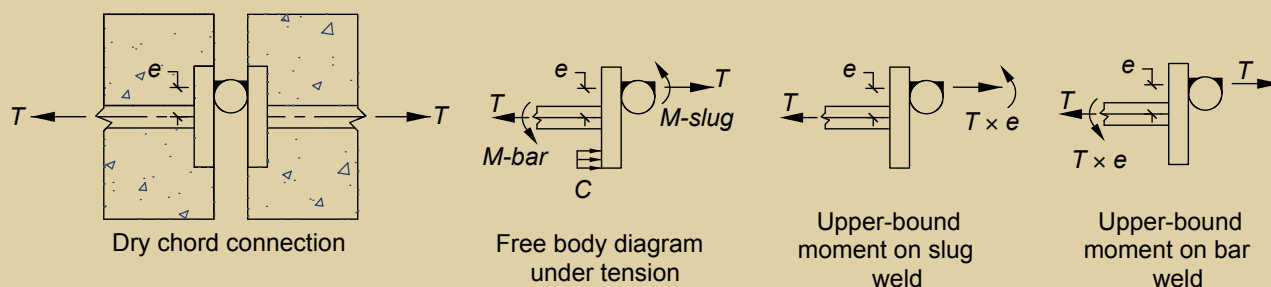


Figure 10. Vertical weld eccentricity often occurs when the slug weld is not in alignment with the center of the chord reinforcement. Note: C = bearing force of the faceplate on the concrete; e = eccentricity between the center of bar and weld; M -bar = flexure in the bar; M -slug = flexure in the slug weld; T = tension forces.

weld and the hairpin bend, the connection will be stiff and yield will occur at small tensile displacement. This behavior can also occur when the slug is not in alignment with the hairpin.

For example, if the slug is offset toward one leg of the hairpin, the connection will behave in a stiff manner and premature weld fracture near the anchorage leg can occur. To increase the joint tensile displacement, the length between the slug and the hairpin bend can be maximized. For example, using the model presented in Fig. 9 and a distance of four bar diameters will provide a tensile opening of about 1.5 in. (38 mm) at yield.

Dry-chord connection (B)

Experimental results indicated that fracture of the chord-to-slug weld can produce an underestimation of tension capacity. An evaluation of the load path through the connection reveals potential sources for underperformance of dry-chord connections. Further evaluation of this mechanism is detailed in work by Cao and Naito.²⁸

Vertical weld offset Vertical weld eccentricity often occurs when the slug weld is not in alignment with the center of the chord reinforcement (Fig. 10). This weld offset produces additional tension demand on the weld due to the generation of flexure. The additional tension has the poten-

tial to initiate premature weld yielding at a tension force less than that determined from the material yield capacity of the bar. A free body diagram of the connection is presented in Fig. 10. The tension forces T at eccentricity e are resisted by a bearing force of the faceplate on the concrete C or flexure in the slug weld M -slug or flexure in the bar M -bar. As an upper-bound demand on the slug weld, the assumption can be made that all of the flexure is resisted at the slug weld (Fig. 10). This additional flexure can amplify the tension demand on the connection by an order of magnitude. A similar exercise can be conducted by assuming that all of the flexure is resisted by the bars as shown in Fig. 10. The upper-bound weld stress amplification factor AF is computed by neglecting concrete bearing resistance and the bar flexural resistance as in Eq. (3).

$$AF = \frac{\left(\frac{T}{l_w t_w} + \frac{(Te)c}{I} \right)}{\frac{T}{l_w t_w}} \quad \text{Eq. (3)}$$

where

T = tension force

l_w = weld length

t_w = effective throat thickness

e = eccentricity between the center of bar and weld

c = distance between the extreme fiber and center of the weld throat

I = weld moment of inertia about its long axis

A weld offset of $7/16$ in. (11 mm) in connection B can result in a stress amplification factor up to 17.7 at the extreme fiber of the weld, as shown in Fig. 11. Hence, the actual yield capacity of the weld is drastically compromised by a small amount of weld offset. Experimental observations indicate that the weld fracture propagated from the ends of the slug as opposed to from the bottom of the weld. Thus, it is unlikely that vertical offset alone led to the premature

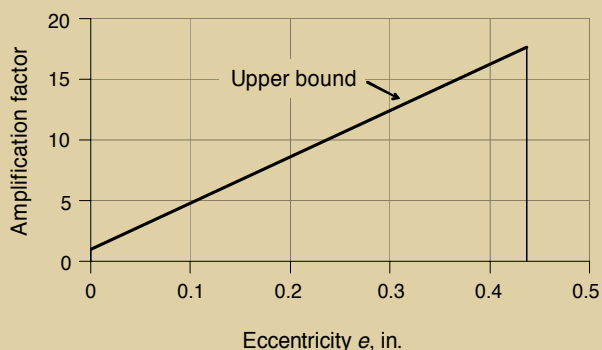


Figure 11. This graph compares the eccentricity with the amplification factor. Note: 1 in. = 25.4 mm.

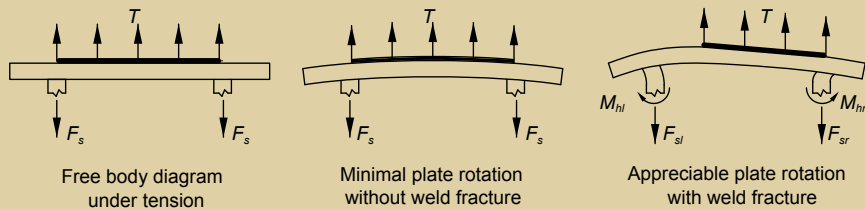


Figure 12. These diagrams and the photo show the plate flexural deformation from the plan view. Note: F_s = tension demand in bar; F_{sl} = tension demand in left bar; F_{sr} = tension demand in right bar; M_{nl} = moment demand in left bar; M_{nr} = moment demand in right bar; T = tension on slug weld.

weld failure in the tension tests.

Nevertheless, minor vertical offset can result in a considerable amplification of demands on the weld. Considering the possibility of vertical weld offset between two unlevelled, double-tee flanges in the field, specific eccentricity limits should be prescribed in the construction documents and inspection should be conducted to verify that the tolerances are maintained. Development of eccentricity limits is dependent on the geometry of the faceplate, chord bar, and weld used and should be part of the chord-design process.

In-plane plate flexure Fracture of the slug-to-plate weld or in-plane construction errors can instigate a progressive failure of the connection. Once fracture of the weld initiates, appreciable bending deformation of the connection faceplate can occur (Fig. 12). This eccentric plate rotation produces flexural demands on the anchorage-bar connection on the back of the faceplate. The combination of flexure and tension results in a premature failure of the anchorage bars. This behavior was observed in connection B, where fracture of the slug weld initiated a brittle fracture in the left bar followed by a ductile fracture in the right bar (Fig. 13).

The welded-chord-connection tension capacity is dependent on the performance of slug-to-plate weld. To achieve the tension strength of anchorage bars, the slug-to-faceplate weld must be oversized to preclude any bar bending. Precautions should be taken to minimize the vertical eccentricity and horizontal plate flexure with special attention paid to the weld alignment. As an alternative, a pour strip or cover plate can be used for reliable tension transfer.

Conclusion

Precast concrete double-tees use one of five categories of connections for shear or tension transfer between panels. An experimental research program examined the tension performance of seven connections representative of these categories and commonly used in current U.S. construction. From the test observations and measurements and dis-

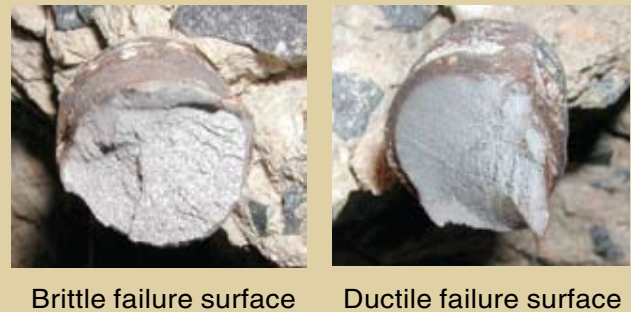


Figure 13. Fracture of the slug weld initiated a brittle fracture in the left anchorage bar followed by a ductile fracture in the right anchorage bar.

cussions presented, the following conclusions are drawn:

Hairpin connections are capable of resisting moderate tension demands over a significant deformation range. The tension yield and ultimate resistance provided by these connections does not conform to the truss analogy. To determine a tension capacity of the connection, a simplified beam analogy is developed and shown to provide a good estimate of the yield capacity. Using the formulation developed, the contribution of web connections to diaphragm flexural resistance can be determined.

The dry-welded chord connection exhibited premature tensile failure due to fracture at the slug weld. Modification of the weld detail in combination with minimized vertical and in-plan offsets on the slug could provide a more robust connection. To achieve the connector capacity, the welds should be oversized and all field welding should be examined to ensure that eccentricities are within the predetermined allowances.

The pour-strip chord connection exhibited a high deformation capacity and achieved its nominal strength.

The topped cover plate provides a stiff connection capable of developing the tensile strength of the anchorage bars. The connection is sensitive to combined shear demands and may not achieve the tension capacity under these conditions.

The use of 2-in.-thick (50 mm) topping on a 2-in.-thick precast concrete section with ¼ in. (6.25 mm) of roughness and WWR spaced at 10 in. (250 mm) achieves the expected strength but at a low deformation level. Fracture of the WWR occurs prior to 0.2 in. tensile displacement due to the material properties of the cold-worked wire.

Accounting for the strength of WWR in the diaphragm resistance is dependent on the stiffness of other connections. Use of stiff chord and web connections will limit the tensile deformation capacity of the joint and allow the strength of WWR to remain effective. Use of flexible web and chord connections, however, may cause the WWR to fracture prior to activation of the embedded mechanical connections.

Acknowledgments

This research is part of a collaborative research project sponsored by PCI and the National Science Foundation (CMS-0324522). In addition, the project has support from a grant from the Commonwealth of Pennsylvania Department of Community and Economic Development through the Pennsylvania Infrastructure Technology Alliance. The authors thank Richard Sause and Robert Fleischman for guidance and consultation and the Diaphragm Seismic Design Methodology advisory board for development and review of the research program.

References

1. PCI Industry Handbook Committee. 2004. *PCI Design Handbook: Precast and Prestressed Concrete*. 6th ed. Chicago, IL: PCI.
2. Fleischman, R. B., R. Sause, S. Pessiki, and A. B. Rhodes. 1998. Seismic Behavior of Precast Parking Structure Diaphragms. *PCI Journal*, V. 43, No. 1 (January–February): pp. 38–53.
3. Fleischman, R., C. Naito, J. Restrepo, R. Sause, and S. Ghosh. 2005. Precast Diaphragm Seismic Design Methodology (DSDM) Project, Part 1: Design Philosophy and Research Approach. *PCI Journal*, V. 50, No. 5 (September–October): pp. 68–83.
4. Fleischman, R. B., C. Naito, J. Restrepo, R. Sause, S. K. Ghosh, G. Wan, M. Schoettler, and L. Cao. 2005. Precast Diaphragm Seismic Design Methodology (DSDM) Project, Part 2: Research Program. *PCI Journal*, V. 50, No. 6 (November–December): pp. 14–31.
5. Naito, C., and L. Cao. 2004. Precast Diaphragm Panel Joint Connector Performance. Paper 2722. In *Proceedings 13th World Conference on Earthquake Engineering*. Vancouver, Canada: 13th World Conference on Earthquake Engineering,
6. Venuti, William J. 1970. Diaphragm Shear Connectors between Flanges of Prestressed Concrete T-Beams. *PCI Journal*, V. 15, No. 1 (February): pp. 67–78.
7. Concrete Technology Corp. 1974. *Tests of Shear Connectors Report*. CTA-74-B8/9, pp. 55–62. Tacoma, WA: Concrete Technology Corp.
8. Aswad, A. 1977. *Comprehensive Report on Precast and Prestressed Connections Testing Program*. Denver, CO: Stanley Structures Inc.
9. Spencer, R. 1986. Earthquake Resistant Connections for Low Rise Precast Concrete Buildings. In *Seminar on Precast Concrete Construction in Seismic Zones*. V. 1. NSF/Japan Society for the Promotion of Science. Tokyo, Japan: Japan Concrete Institute.
10. Kallros, M. K. 1987. An Experimental Investigation of the Behavior of Connections in Thin Precast Concrete Panels under Earthquake Loading. M.S. thesis. Civil Engineering Department, University of British Columbia in Canada.
11. Pincheira, J. A., M. G. Oliva, and F. I. Kusumohardjo. 1998. Tests on Double Flange Connectors Subjected to Monotonic and Cyclic Loading. *PCI Journal*, V. 43, No. 3 (May–June): pp. 82–96.
12. Oliva, M. G. 2000. Testing of the JVI Flange Connector for Precast Concrete Double-Tee Systems. Structures and Materials Test Laboratory, University of Wisconsin, Madison, WI.
13. Shaikh, A. F., and E. P. Feile. 2002. Testing of JVI Vector Connector. University of Wisconsin, Milwaukee, WI.
14. Wiss, Janney, Elstner Associates Inc. 2002. Dayton/Richmond Flange-to-Flange Connector Tests. Miamisburg, OH: Wiss, Janney, Elstner Associates Inc.
15. Pincheira, J. A., M. G. Oliva, and W. Zheng. 2005. Behavior of Double-Tee Flange Connections Subjects to In-Plane Monotonic and Reversed Cyclic Loads. *PCI Journal*, V. 50, No. 6 (November–December): pp. 32–54.
16. Naito, C., W. Peter, and L. Cao. 2006. *Development of a Seismic Design Methodology for Precast Diaphragms—Phase 1 Summary Report*. ATLSS report no.06-03. Bethlehem, PA: ATLSS Center, Lehigh University.

17. American Concrete Institute (ACI) Committee 318. 2002. *Building Code Requirements for Structural Concrete (ACI 318-02) and Commentary (ACI 318R-02)*. Farmington Hills, MI: ACI.
18. American Welding Society (AWS) Structural Welding Committee. 1992. *Structural Welding Code—Reinforcing Steel*. AWS D1.4-1992. Miami, FL: AWS.
19. American Society for Testing and Materials (ASTM) A304. 2005. *Standard Specification for Carbon and Alloy Steel Bars Subject to End-Quench Hardenability Requirements*. West Conshohocken, PA: ASTM.
20. ASTM C39. 2005. *Standard Test Method for Compressive Strength of Cylindrical Concrete Specimens*. West Conshohocken, PA: ASTM.
21. ASTM A36. 2008. *Standard Specification for Carbon Structural Steel*. West Conshohocken, PA: ASTM.
22. ASTM A185. 2007. *Standard Specification for Steel Welded Wire Reinforcement, Plain, for Concrete*. West Conshohocken, PA: ASTM.
23. ASTM A706. 2008. *Standard Specification for Low-Alloy Steel Deformed and Plain Bars for Concrete Reinforcement*. West Conshohocken, PA: ASTM.
24. AWS Structural Welding Committee. 2004. *Structural Welding Code—Steel*. AWS D1.1-2004. 19th ed. Miami, FL: AWS.
25. Priestley, M. J. N. 1992. The U.S.-PRESSS Program Progress Report. In *Third Meeting of the U.S.-Japan Joint Technical Coordinating Committee on Precast Seismic Structural Systems*. JTCC-PRESSS. San Diego, CA.
26. Building Seismic Safety Council. 1997. *NEHRP Guidelines for the Seismic Rehabilitation of Buildings*. FEMA publication 273. Washington, DC: FEMA.
27. Mirza, S. A., and J. G. MacGregor. 1981. Strength and Ductility of Concrete Slabs Reinforced with Welded Wire Fabric. *ACI Journal*, V. 78, No. 5 (September–October): pp. 374–81.
28. Cao, L., and C. Naito. 2007. Design of Precast Diaphragm Chord Connections for In-Plane Tension Demands. *ASCE Journal of Structural Engineering*, V. 133, No. 11 (November): pp. 1627–1635.

Notation

A_s	= cross-sectional area of one leg of the connection
A_{wwr}	= total cross-sectional area of welded-wire reinforcement crossing the joint
AF	= upper-bound weld stress amplification factor
c	= distance between the extreme fiber and center of the weld throat
C	= bearing force of the faceplate on the concrete
d	= diameter of the reinforcing bar
e	= eccentricity between the center of bar and weld
f_u	= reinforcing bar ultimate tensile strength
f_{wwr}	= welded-wire reinforcement yield strength
f_y	= reinforcing bar yield strength
F_s	= tension demand in bar
F_{sl}	= tension demand in left bar
F_{sr}	= tension demand in right bar
F_y	= yield stress of the reinforcing bar
I	= weld moment of inertia about its long axis
K_t	= tension stiffness
l_w	= weld length
L	= distance from end of slug weld to bar end
M_{hl}	= moment demand in left bar
M_{hr}	= moment demand in right bar
M_p	= plastic moment
$M\text{-bar}$	= flexure in the bar
$M\text{-slug}$	= flexure in the slug weld
P_n	= estimated strength
P_{ult}	= ultimate strength
t_w	= effective throat thickness
T	= tension forces

- T_a = tension resistance at point a
- T_b = tension resistance at point b
- T_c = tension resistance at point c
- T_y = yield strength of the connection
- V = shear in hairpin at yield
- δ_t = tension displacement
- δ_v = shear displacement

About the authors



Clay Naito, PhD, is an associate professor for the Department of Civil and Environmental Engineering at Lehigh University in Bethlehem, Pa.



Liling Cao, PhD, is a senior engineer with Thornton Tomasetti in Philadelphia, Pa.



Wesley Peter, MSCE, works for SK&A Consulting Structural Engineers in Washington, D.C.

Synopsis

An experimental study of flange-to-flange connections of double-tees was conducted as part of the PCI-funded research effort in developing a seismic design methodology for precast concrete diaphragms. The research program categorizes the strength and deformation capacity of common double-tee flange and chord connections under monotonic and cyclic loading.

This paper focuses on the tension response of connections compared with design expectations and the contribution they provide in flexural resistance of the diaphragm. The pretopped flange connections were found to resist a moderate tensile force over a large deformation range. Flange connections in topped-diaphragm systems provided a high initial tensile resistance but returned to the untopped response once the topping reinforcement failed. The strengths of both chord and flange connections were overpredicted by PCI equations due to brittle modes of weld failure. Consequently, attention should be paid to field weld alignment, and simplified models were developed to more accurately estimate the deformation capacity and strength.

Keywords

Chord, connection, diaphragm, double-tee, flange connection, seismic, tension response, testing, web, welded-wire reinforcement, WWR.

Review policy

This paper was reviewed in accordance with the Precast/Prestressed Concrete Institute's peer-review process.

Reader comments

Please address any reader comments to *PCI Journal* editor-in-chief Emily Lorenz at elorenz@pci.org or Precast/Prestressed Concrete Institute, c/o *PCI Journal*, 209 W. Jackson Blvd., Suite 500, Chicago, IL 60606. 